

Resorption process in *Astypalaea Linea* extensive region (Europa)

Loïc Mével*, Eric Mercier*

*Laboratoire de Planétologie et Géodynamique, UMR-CNRS 6112
Faculté des Sciences, 2 chemin de la Houssinière, BP 92208, 44322 Nantes cédex 3, France

Correspondence to: loic.mevel@nantes.fr
Eric.Mercier@univ-nantes.fr

Received 9 April 2004; received in revised form 19 October 2004; accepted 16 December 2004.
Planetary and Space Science 53 (2005) 771-779.
www.elsevier.com/locate/pss

Abstract

Whereas numerous extensive features, where new crust is created, are now well recognized on Europa's surface, those relevant to crust disappearance remain difficult to find. This work presents a reconstruction of the surface prior to *Astypalaea Linea*'s emplacement (one of the features where new crustal material appears). We demonstrate that a scattered disappearance of crust takes place in an extensive region close to *Astypalaea Linea*. Physical processes invoked for disappearance are discussed: pressure melting may be responsible for the mobilization of surface material and its collapse down through the icy crust.

Keywords: Europa; Icy satellites; Tectonics; Compression; Morphology; *Astypalaea Linea*; Galileo

1. Introduction

Europa, second and smallest galilean satellite (~1561 km in radius; Davies et al., 1998), is a differentiated body probably composed of a core overlaid with a silicate mantle, itself surrounded by an external H₂O layer ranging from 105 to 140 km depth (Kuskov and Kronrov, 2003). Because of an average equatorial temperature of ~106 K (Spencer et al., 1999), Europa's surface consists in an icy crust. However, jovian tidal heat dissipation may preserve a liquid water ocean under the icy crust and allow internal dynamics (e.g. Ojakangas and Stevenson, 1989; McKinnon, 1999; Ruiz and Tejero, 2003; Tobie et al., 2003). The small impact crater density commonly implies a young mean surface age ranging from 30 to 70 Myr (Zahnle et al., 2003) and then a resurfacing rate similar to those of the Earth's oceanic crust. Analysis of the *Voyager 2* and *Galileo* high resolution images points out the areas of newly created crust associated with correlating displacements of the surrounding crustal blocks (Schenk and McKinnon, 1989; Pappalardo and Sullivan, 1996; Sullivan et al., 1998; Hoppa et al., 1999; Tufts et al., 1999, 2000). Considering a constant Europa's surface, resorption of crust is expected. Features compensating crust extension have yet been proposed by different authors (Sarid et al., 2002; Patterson and Pappalardo, 2002; Greenberg, 2004), however they are not sufficient to explain the recorded surface extension and the resorption processes remain ambiguous. Whereas Patterson and Pappalardo (2002) and Patterson et al. (2004) shown that oblique compression occurs along prominent and well-defined ridges in *Castalia Macula* region, Sarid et al. (2002) and Greenberg (2004) found that strike-slip motions could be associated to convergence along bands having "muscle tissue" morphologies (i.e. similar to extensive bands textures such as *Astypalaea Linea*).

This study points out the discovery of crust resorption in the extensive region of *Astypalaea Linea*. This scattered phenomenon implies a great number of elementary ridge-like structures and represents a new compressive style from a morphological point of view. We will consequently discuss the physical processes that may be responsible for this crust disappearance.

2. The studied area: *Astypalaea Linea* region

Astypalaea Linea is a 810 km long or more linear feature discovered on *Voyager 2* images, oriented NNW-SSE and extending from 60°S & 191.1°W probably down to the south pole (Tufts et al., 1999). During the E17 orbit, *Galileo*'s SSI (Solid State Imaging) camera provided high resolution images of its north portion (fig. 1). Each image is numbered from 1 to 9 northward.

Three categories of features with different stratigraphic ages are observed on the mosaic (fig. 1): 1) complex rugged terrains including an entanglement of ridges, depressions and fractures, 2) a dark finely striated band (*Astypalaea Linea*) clearly cutting across the more ancient ridged terrains and, 3) four thick ridges named *flexi* and tens of fractures cutting across *Astypalaea* without deformations postdate the band.

Astypalaea is composed of three rhomboidal lenses oriented N-S (segments 1 to 4 on fig. 1), whose morphology suggests a pull-apart style opening. A large area named *Cyclades Macula* terminates the band to the north and a fourth rhomboidal lens similar to the others extends the band to the south (fig. 1). This regional feature indicates a N-S extensional dextral movement of about 60 km (Sylvester, 1988; Tufts et al., 1999). Whatever the kinematics of *Astypalaea* opening, a reconstitution of its initial state (before the band emplacement) by using piercing points (i.e. ridges, troughs, furrows) distributed along the band should be possible.

3. Reconstruction of the initial state (*ante-Astypalaea Linea*)

3.1. Correction of images

All nine high-resolution *Galileo* images have been normalized and scaled to the image 9 (the nearest image from *Galileo* spacecraft) in order to minimize errors on the reconstructions and on the measurements of distances and areas. Figure 2a shows that horizontal resolution increases almost linearly along the mosaic. Then we compute distortion coefficients (β) on both horizontal and vertical resolutions (respectively, r_h and r_v) on each image except the image 9, which is the reference (r_{href} and r_{vref}), as follows:

$$\beta_h = \frac{r_h}{r_{href}} \quad \text{and} \quad \beta_v = \frac{r_v^2}{r_{vref} r_{href}} \quad (3.1)$$

in order to obtain the same 48 m.pixel^{-1} resolution everywhere on the mosaic. The borders of the resulting mosaic are compared to the mosaic before correction on fig. 2b. Contrary to an orthographic projection, this type of correction does not preserve angles, but has the advantage to preserve distances and areas. Then we prefer this type of correction because *Astypalaea Linea* is a linear feature oriented N-S. The error on the angles is consequently small and the distances are valuable.

3.2. Reconstruction method

Cutting off the band from the mosaic, a set of blocks carrying piercing points at both east (E) and west (W) can be defined (fig. 3a). Reconstruction of the surface state prior to *Astypalaea* emplacement should be possible by restoring continuities on 34 pre-existing structures (black lines on fig. 3a) distributed on both margins of the band. An example is well illustrated in the box b on fig. 3 by closing together areas delimited by the black frames of fig. 3a. In fact, this reconstruction is not easy because of the varying strike-slip amplitude indicated by piercing points along *Astypalaea* (between 65 km and 56 km, fig. 3c). The offset variation is clearly non-linear and cannot depend on the correction method (see fig. 2a).

As shown on fig. 4, this variation could be explained either by divergence (creation of new surface) or by convergence (resorption of ancient surface) in the marginal blocks.

In the case of new material emplacement, dark striated textures typical of extensional zones (Pappalardo and Sullivan, 1996; Sullivan et al., 1998; Tufts et al., 2000) and particular geometry of piercing points are expected (fig. 4a). However, in the case of a lack of ancient material, characteristic offsets of some piercing points must be observed (fig. 4a and b).

We have tested this theory in an area of the mosaic where offset variation between piercing points is important. Figure 5 shows the reconstructed initial surface by using both 5W and 3E blocks. The interpreted sketch (fig. 5d) highlights the necessity to open gaps in the ancient ridged terrains to preserve the continuity of various piercing points. According to the textural and geometrical arguments noted above, no new crustal material is observed around *Astypalaea*, and piercing points offsets and relationships, like those of fig. 4a and b, exist at different places. Then the gaps on the reconstruction represent a crustal resorption during *Astypalaea* opening.

3.3. Application to *Astypalaea Linea*

Extending this procedure to the entire band by using all the major piercing points of fig. 3, we obtain a reconstruction of the initial surface state of *Astypalaea* region as seen on fig. 6. The gaps in the ridged terrains suppose that the recorded surface variation at the

mosaic scale reaches values of about -8 %. The total area of the three rhomboidal lenses is about 3720 km² compared to the area of these gaps, which is about 402 km² (~10.8 % of the lenses surface). In our opinion, this discrepancy is not a problem at all, because surface variation at a given place could be balance everywhere on the spherical surface of the satellite and can extend far away from the band where resolution is too low to detect it. Furthermore, our estimation is a lower limit to the resorption process, which is partly not observable as demonstrated below.

The reconstruction on fig. 6 has been realized by using large piercing points homogeneously distributed along the studied polygon. However, small-scale areas containing second order piercing points exist, as shown in fig. 7a (located on fig. 3b). A set of single ridges, spaced of about 1 km and almost perpendicular to the band orientation, disturbs some older ridges. A detailed reconstruction of this zone points out the convergent style of the deformation and reveals again disappearance of crust never seen on the regional reconstruction (compare fig. 7b, located on fig. 6b, with fig. 7c). Whereas the shortening obtained on fig. 7b reaches only -2.7 %, the shortening obtained by taking into account the second-order piercing points at small-scale (fig. 7c) reaches -13.7 %. This discrepancy shows that the shortening on the regional reconstruction can locally be underestimated by a factor 5.

Whereas creation of crust associated to crustal blocks displacement is common on Europa, our results represent another evidence for massive recycling processes. The scattered distribution of the convergent zones along the band provides a major obstacle to their identification and quantification.

4. Discussion and conclusions

Compressive features have recently been proposed elsewhere on Europa (see section 1). Morphologies associated to these features strongly change from a “muscle tissue” texture as suggested by Sarid et al. (2002) and Greenberg (2004) to a prominent ridge at medium resolution as proposed by Patterson et al. (2004). Our reconstruction suggests that morphology of the compressive features in *Astypalaea Linea* region is mostly characterized by a scattered system of short and subtle ridges (Mével and Mercier, 2002; fig. 7). This morphology represents a new class of compressive features and shows, as conclude Patterson et al., that “muscle tissue” bands are not the only one typical morphologies of compression. The new scattered compressive morphology detected through this work is located near the borders of extensive bands where stresses should be stronger, and indicates that identification and quantification of this type of compression requires, at most, high-resolution image coverage.

Extension and compression lead to two different textural terrains. If one of stage was more recent than the other, we should observe accommodation problems at the boundaries. On the contrary, borders between *Astypalaea Linea* and its surrounding ancient terrains are clearly defined and compressive features apparently do not crosscut these borders. Then, we suggest that extensive and compressive stages are contemporaneous together. It could appear paradoxical to associate the opening of *Astypalaea* with the shortening within its borders. However, the movement along the band does probably hide complex kinematics controlled by a cyclic incremental process (extension, right lateral strike-slip, compression, left lateral strike-slip) materialized by alternative ridges and troughs, and resulting from diurnal tide variations (Hoppa et al., 1999). In this way, Prockter and Pappalardo (2000) have discovered a set of folds inside the band (lenses 3 and 4 on fig. 1b), which may result from late transpressive movements along *Astypalaea* (i.e. folding during the compression and left lateral strike-slip stages according to the opening process invoked by Hoppa et al., 1999).

Then, the N-S compressive context around *Astypalaea* suggested by crust disappearance could be compatible with the compressive component produced during band working.

Shortening measured on images does not compensate all the observed extension on *Astypalaea*. However, the data set was focused on major features like *Astypalaea Linea*. Consequently, these images might not be characteristic of the Europa's surface and crust disappearance occurs strongly outside the studied area.

Several mechanisms could explain this disappearance. The Earth's oceanic crust cycle produces large-scale features like subduction zones and their associated ocean trenches. Nevertheless, the lack of significant scraps on Europa and the large ice rigidity (due to the low surface temperatures) do not fit with the existence of overlapping-type processes occurring over the entire crustal thickness along compressive ridges.

Another possible mechanism could be melting under pressure. However, it requires some constraints on temperature, pressure, and composition of the icy material. The most unfavourable temperature conditions to melt are those found on the surface (ranging from 86 K to 132 K according to Spencer et al., 1999). In contrast with "lithostatic" pressure, which is weaker at shallow depth, the order of magnitude of tectonic stresses remains unknown. Despite this uncertainty, melting of pure water ice is impossible below 250 K (Chizhov, 1993). However, mixed compounds decrease the water liquidus temperature (fig. 8).

The *Galileo's* Near-Infrared Mapping Spectrometer (NIMS) provides chemical compositions of the surface indicating the presence of magnesium ($\text{MgSO}_4 \cdot n\text{H}_2\text{O}$), sodium ($\text{Na}_2\text{SO}_4 \cdot n\text{H}_2\text{O}$, $\text{Na}_2\text{CO}_3 \cdot n\text{H}_2\text{O}$) (McCord et al., 1998) and/or sulphuric acid hydrates ($\text{H}_2\text{SO}_4 \cdot n\text{H}_2\text{O}$) (Carlson et al., 1999) mixed with water ice. These compounds offset the ice liquidus toward lower temperatures but, despite uncertainties on stresses, the liquidus temperature remains still much larger than surface temperatures (Zelevnik, 1991; Hogenboom et al., 1995; Grasset et al., 2001; Hogenboom et al., 2001; Kargel et al., 2001). The most efficient compound to decrease the water liquidus temperature is ammonia. Even if the NIMS didn't observe it, models of icy satellites formation (e.g. Lewis, 1971; Mousis et al., 2002) systematically predict its presence in depth. Evolution of the liquidus as a function of the ammonia weight rate shows that the eutectic composition provides the melting at ~ 177 K under pressures up to 200 MPa (Grasset et al., 1995; Hogenboom et al., 1997; see fig. 8).

Still, surface temperatures remain too small: even with the most favourable assumptions on the chemistry or the tectonic pressures exerted in the crust, melting of the ice cannot be obtained, unless an additional heat source is supplied. This last assumption may be achieved since *Astypalaea Linea* is a centre of crust creation by deep warm material upwelling, implying a positive thermal anomaly in the area. Another hypothesis may be that movements induced by diurnal tidal effects (see the scenario of Hoppa et al., 1999) generate viscous frictions increasing locally heat dissipation (Nimmo and Gaidos, 2002). Both processes may act together and melt the crust under stresses at shallow depth. The produced liquid would be enriched in hydrates and denser than ice, but part of it may rise under pressure according to the diurnal tidal variations of the stresses pattern. The pads constituting of the compressive ridges (e.g. fig. 7) may then result from accumulation of remnants not sublimed at the surface. Unfortunately, no sufficiently high-resolution spectral data allows correlation between structures and composition on the surface near *Astypalaea*. Thus, the physical origin of crustal resorption remains problematic.

In summary, the proposed reconstruction shows that extension observed along the stratigraphically recent *Astypalaea* dark band is partly compensated by a weakly localized disappearance of crustal material among the surrounding ancient ridged plains. We suggest that this process should be more efficient and spatially more extended than our mosaic-scale reconstruction, and that it can totally compensate the crust creation recorded on Europa's

surface. Although the physical mechanism responsible for these observations still cannot be strictly identified, pressure melting accommodated with an additional heat source (provided by viscous friction or local thermal anomalies) seems to be a good candidate. In this way, crustal recycling zones on Europa would be associated to a warm crustal context rather than a cold region like the Earth subduction zones.

Acknowledgements

Thanks to the reviewers, Christophe Sotin and Gaël Choblet for their helpful discussions, which have greatly contributed to improve this study. Thanks to Alain Cossard for the quality of the figures. This work was supported by the INSU Programme National de Planétologie.

References

- Carlson, R.W., Johnson, R.E., Anderson, M.S., 1999. Sulfuric acid on Europa and the radiolytic sulfur cycle. *Science* 286, 97-99.
- Chizhov, V.E., 1993. Thermodynamic properties and equation of state of high-pressure ice phases. Translated from *Prikladnaya Mekhanika Tekhnicheskaya Fizika* 2, 113-123 (translation).
- Davies, M.E., et al., 1998. The control networks of the Galilean satellites and implications for global shape. *Icarus* 135, 372-376.
- Grasset, O., Beauchesne, S., Sotin, C., 1995. Investigation of the NH₃-H₂O phase diagram in the range 100 MPa-1.5 GPa using *in situ* Raman spectroscopy: application to Titan's dynamics. *Compt. Rend. Acad. Sci. II* 320, 249-256.
- Grasset, O., Mével, L., Mousis, O., Sotin, C., 2001. The pressure dependence of the eutectic composition in the system MgSO₄-H₂O: implications for the deep liquid layer of icy satellites. *Proc. Lunar Planet. Sci. Conf. 32*, #1524, Houston, Texas.
- Greenberg, R., 2004. The evil twin of Agenor: tectonic convergence on Europa. *Icarus* 167, 313-319.
- Hogenboom, D.L., Kargel, J.S., Ganasan, J.P., Lee, L., 1995. Magnesium sulfate-water to 400 MPa using a novel piezometer: densities, phase equilibria, and planetological implications. *Icarus* 115, 258-277.
- Hogenboom, D.L., Kargel, J.S., Consolmagno, G.J., Holden, T.C., Lee, L., Buyyounouski, M., 1997. The ammonia-water system and the chemical differentiation of icy satellites. *Icarus* 128, 171-180.
- Hogenboom, D.L., Kargel, J.S., Daly, M.E., 2001. Stable and metastable high pressure phases of the sulfuric acid - magnesium sulfate - water system: applications to Europa. *Proc. Lunar Planet. Sci. Conf. 32*, #1739, Houston, Texas.
- Hoppa, G., Tufts, B.R., Greenberg, R., Geissler, P., 1999. Strike-slip faults on Europa: global shear patterns driven by tidal stress. *Icarus* 141, 287-298.

- Kargel, J.S., Head, J.W., Hogenboom, D.L., Khurana, K.K., Marion, G., 2001. The system sulphuric acid - magnesium sulfate - water: Europa's ocean properties related to thermal state. Proc. Lunar Planet. Sci. Conf. 32, #2138, Houston, Texas.
- Kuskov, O.L., Kronrov, V.A., 2003. Chemical differentiation of the Galilean satellites of Jupiter. 2. Interior structure of Europa. *Geochemistry International* 41, 984-1001.
- Lewis, J.S., 1971. Satellites of the outer planets: their physical and chemical nature. *Icarus* 15, 174-185.
- McCord, T.B., Hansen, G., Fanale, F., Carlson, R., Matson, D., Johnson, T., Smythe, W., Crowley, J., Martin, P., Ocampo, A., Hibbitts, C., Granahan, J., and the NIMS Team, 1998. Salts on Europa's surface detected by Galileo's Near Infrared Mapping Spectrometer. *Science* 280, 1242-1245.
- McKinnon, W.B., 1999. Convective instability in Europa's floating ice shell. *Geophys. Res. Lett.* 26, 951-954.
- Mével, L., Mercier, E., 2002. Geodynamics on Europa: Evidence for a crustal resorption process. *Proceedings of the Lunar and Planetary Science Conference*, vol. 32, #1476, Houston, Texas.
- Mousis, O., Gautier, D., Bockélee-Morvan, D., 2002. An evolutionary turbulent model of the saturn's subnebula : implications on the origin of the atmosphere of Titan. *Icarus* 156, 162-175.
- Nimmo, F., Gaidos, E., 2002. Strike-slip motion and double ridge formation on Europa. *J. Geophys. Res.* 107.
- Ojakangas, G.W. and Stevenson, D.J., 1989. Thermal state of an ice shell on Europa. *Icarus* 81, 220-241.
- Pappalardo, R.T. and Sullivan, R.J., 1996. Evidence for separation across a grey band on Europa. *Icarus* 123, 557-567.
- Patterson, G.W., Pappalardo, R.T., 2002. Compression Across Ridges on Europa. *Proceedings of the Lunar and Planetary Science Conference*, vol. 33, #1681, Houston, Texas.
- Patterson, G.W., Head, J.W., Pappalardo, R.T., 2004. Convergent boundaries on Europa: a numerical approach to Euler pole analysis and its implications for plate reconstruction. *Proceedings of the Lunar and Planetary Science Conference*, vol. 35, #1590, Houston, Texas.
- Prockter, L.M. and Pappalardo, R.T., 2000. Folds on Europa: implications for crustal cycling and accommodation of extension. *Science* 289, 941-943.
- Ruiz, J., Tejero, R., 2003. Heat flow, lenticulae spacing, and possibility of convection in the icy shell of Europa. *Icarus* 162, 362-373.
- Sarid, A.R., Greenberg, R., Hoppa, G.V., Tufts, B.R., Geissler, P., 2002. Polar wander and surface convergence of Europa's ice shell: evidence from a survey of strike-slip displacement. *Icarus* 158, 24-41.

- Schenk, P.M. and McKinnon, W.B., 1989. Fault offsets and lateral crustal movement on Europa: evidence for a mobile ice shell. *Icarus* 79, 75-100.
- Spencer, J.R., Tamppari, L.K., Martin, T.Z., Travis, L.D., 1999. Temperatures on Europa from Galileo PhotoPolarimeter Radiometer : Nighttime thermal anomalies. *Science* 285, 150-153.
- Sullivan, R., Greeley, R., Homan, K., Klemaszewski, J., Belton, M., Carr, M., Chapman, C., Tufts, B., Head, J., Pappalardo, R., Moore, J., Thomas, P., and the Galileo SSI Team, 1998. Episodic plate separation and fracture infill on the surface of Europa. *Nature* 391, 371-372.
- Sylvester, A.G., 1988. Strike-slip faults. *Geol. Soc. Am. Bull.* 100, 1666-1703.
- Tobie, G., Choblet, G., Sotin, C., 2003. Tidally heated convection: constraints on Europa's ice shell thickness. *J. Geophys. Res.* 108, 5124.
- Tufts, B.R., Greenberg, R., Hoppa, G., Geissler, P., 1999. Astypalaea Linea: a large-scale strike-slip fault on Europa. *Icarus* 141, 53-64.
- Tufts, B.R., Greenberg, R., Hoppa, G., Geissler, P., 2000. Dilation of the European lithosphere. *Proc. Lunar Planet. Sci. Conf.* 31, #1773, Houston, Texas.
- Zahnle, K.L., Schenk, P., Levison, H.F., Dones, L., 2003. Cratering rates in the outer solar system. *Icarus* 163, 263-289.
- Zeleznik, F.J., 1991. Thermodynamic properties of the aqueous sulfuric acid system to 350 K. *J. Phys. Chem. Ref. Data* 20, 1157-1200.

Figures

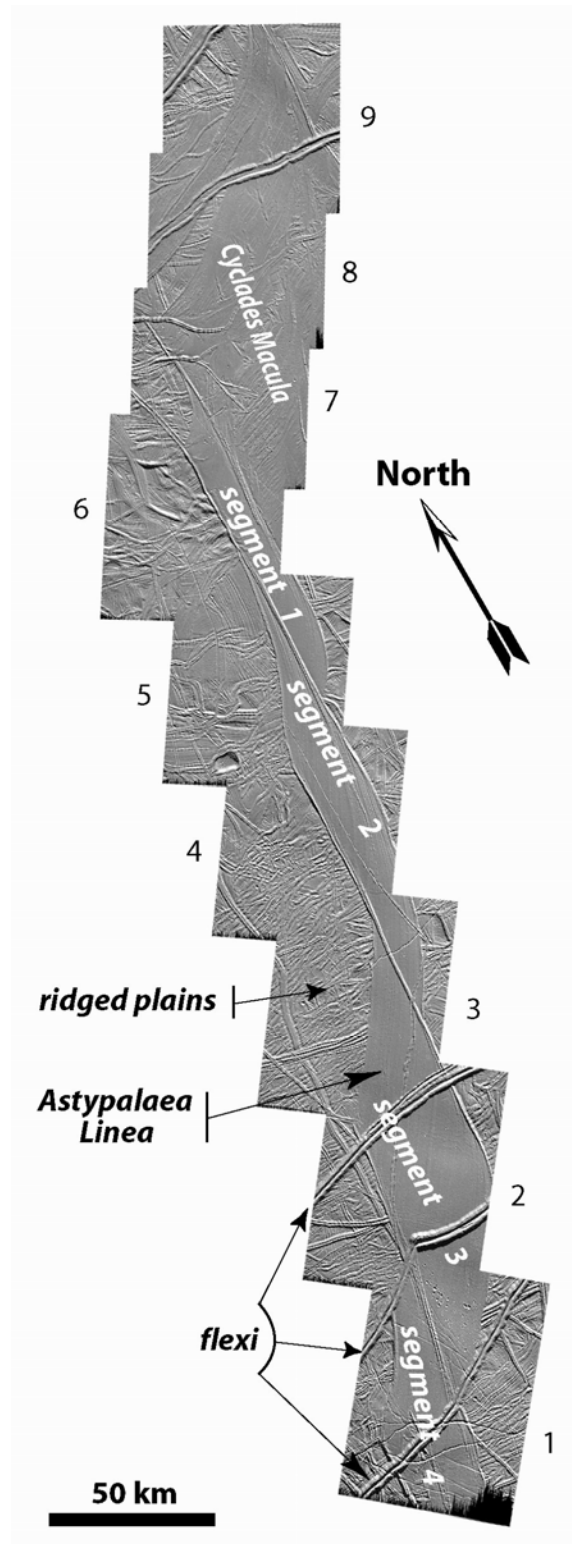


Fig. 1

Mosaic composed of nine high-resolution images ($\sim 50 \text{ m} \cdot \text{pixel}^{-1}$) taken by the *Galileo*'s SSI camera during E17 orbit. These images (17E0061-69), whose resolutions are normalized to the image 9, reveal the 310 km long north end of *Astypalaea Linea*. The high-resolution coverage extends from 61°S & 190°W down to 70°S & 198°W . Localization and nomenclature of large units are indicated.

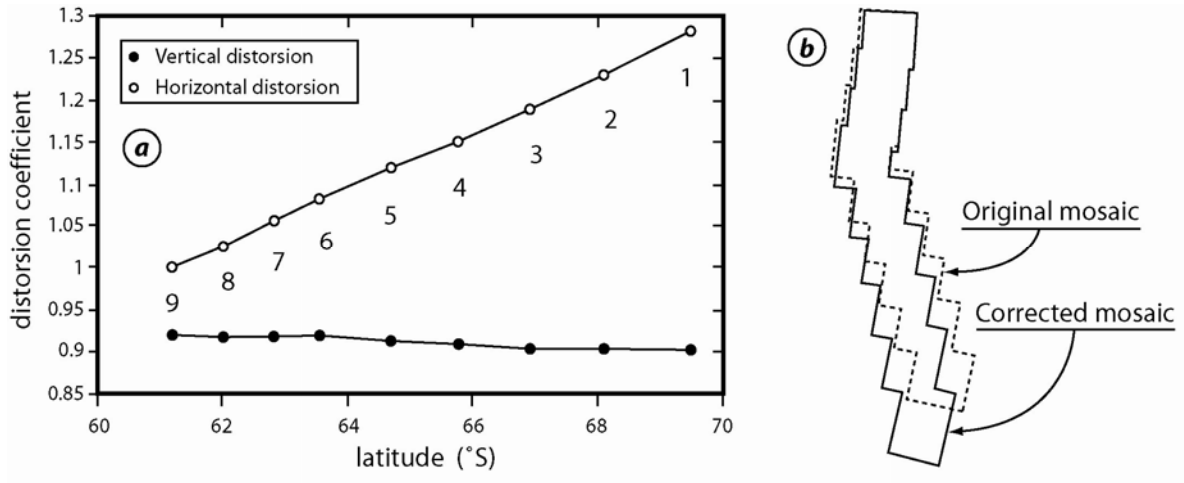


Fig. 2
 (a) Distorsion coefficients as a function of latitude for horizontal and vertical resolutions. Each point represents the centre of an image. Both resolutions have a linear trend. (b) Comparison between the original mosaic (dotted lines) with the corrected mosaic (full lines).

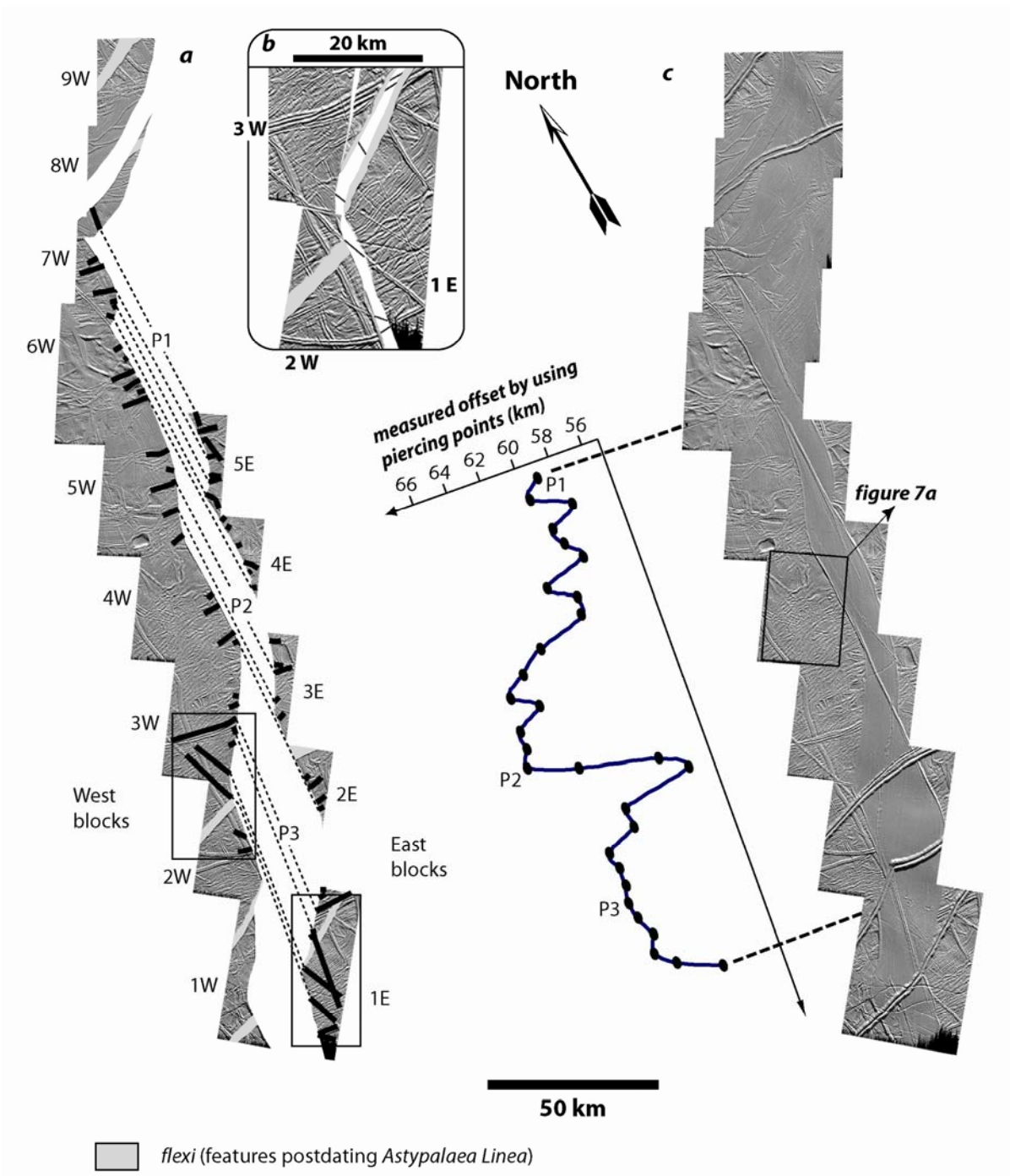


Fig. 3

(a) Removing the band from the mosaic, West and East blocks can be defined. Black lines represent the piercing points displayed on the ancient ridged terrains along *Astypalaea Linea* and used for the reconstruction. The box *b* illustrates the continuity of some piercing points after restoration by using areas defined by both black frames on *a*. Features postdating *Astypalaea Linea* (*flexi*) are greyed. (c) Measured offsets of 30 piercing points (dots on the curve) show a non-linear variation ranging from 56 to 65 km along the band. Dots P1 to P3 refer to the piercing points on mosaic *a*.

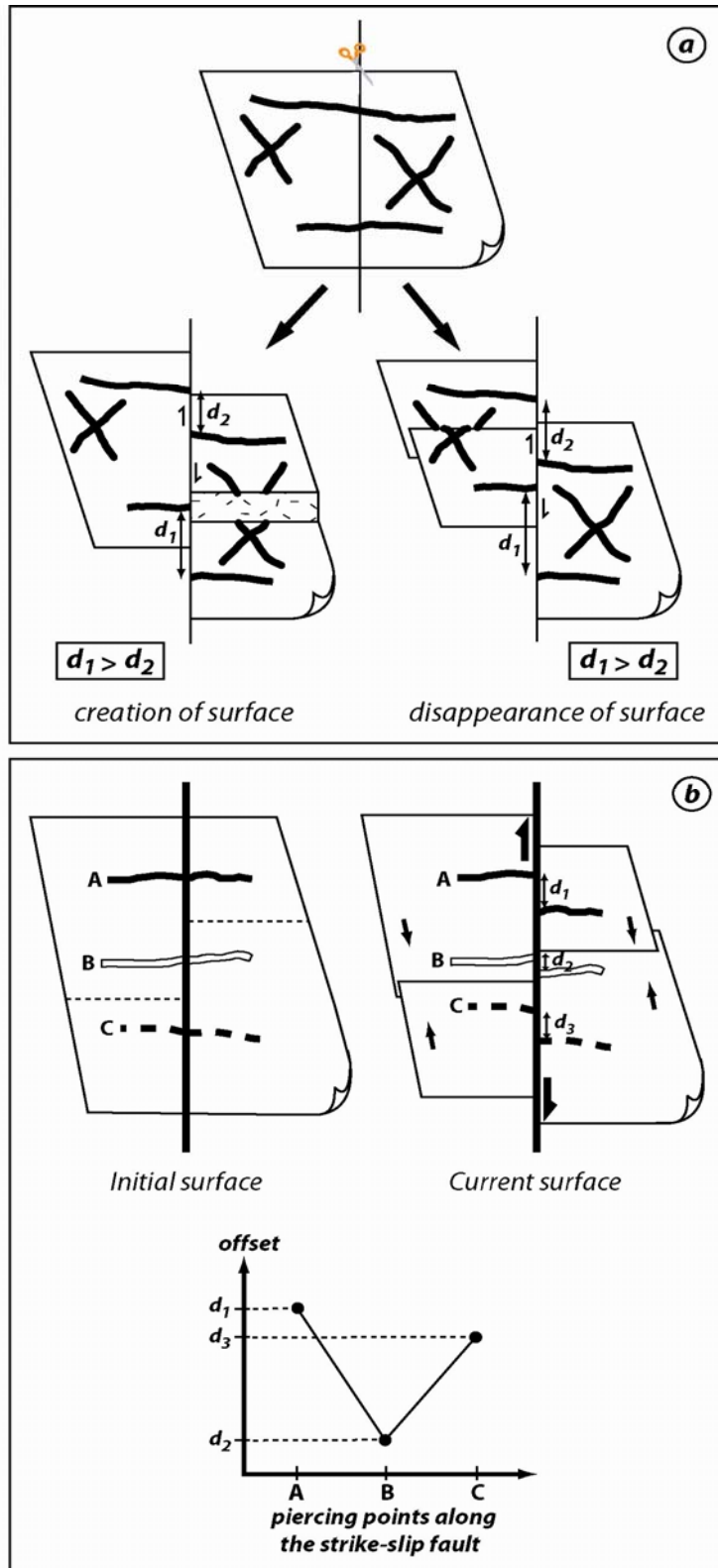


Fig. 4

(a) Theoretical sketches illustrating an offset variation ($d_1 > d_2$) along a dextral strike-slip fault. This may result from either creation or disappearance of surface. (b) Heterogeneous distribution of creation (extension) or disappearance (shortening as illustrated here) zones account for the offset variation along strike-slip fault. The schematic graph shows the offset variation along the strike-slip fault (compare with fig. 3b).

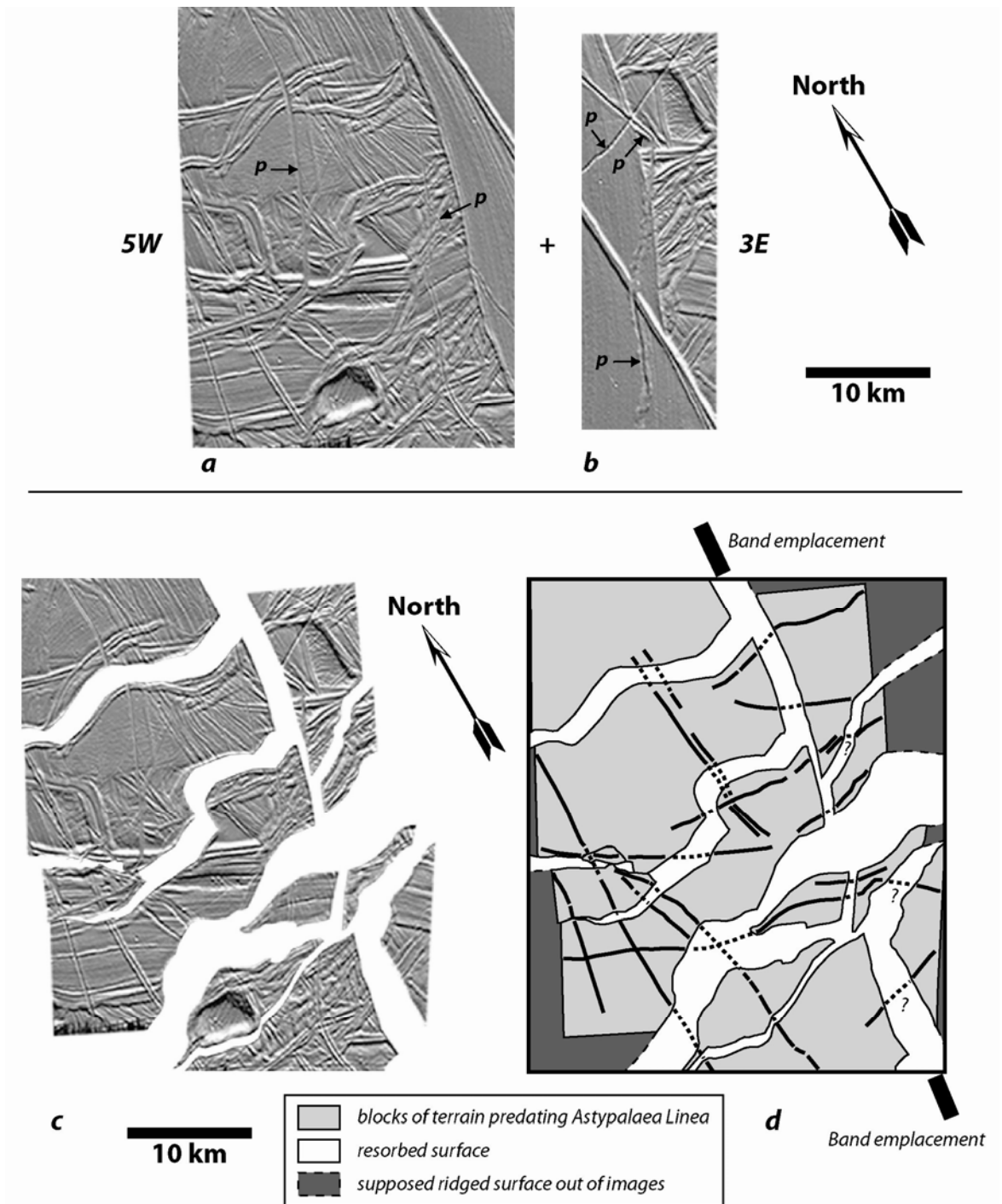


Fig. 5

Reconstructed portion of *Astypalaea Linea* shown in the frames on fig. 6. By restoring continuity of piercing points of various orientations, shortening (gaps) is required on both sides of the band. The initial state of the (a) and (b) images lead to the interpreted sketch (f), where black lines represent the used piercing points. Letters *p* on images (a) and (b) report to features postdating *Astypalaea Linea* and are consequently not used here.

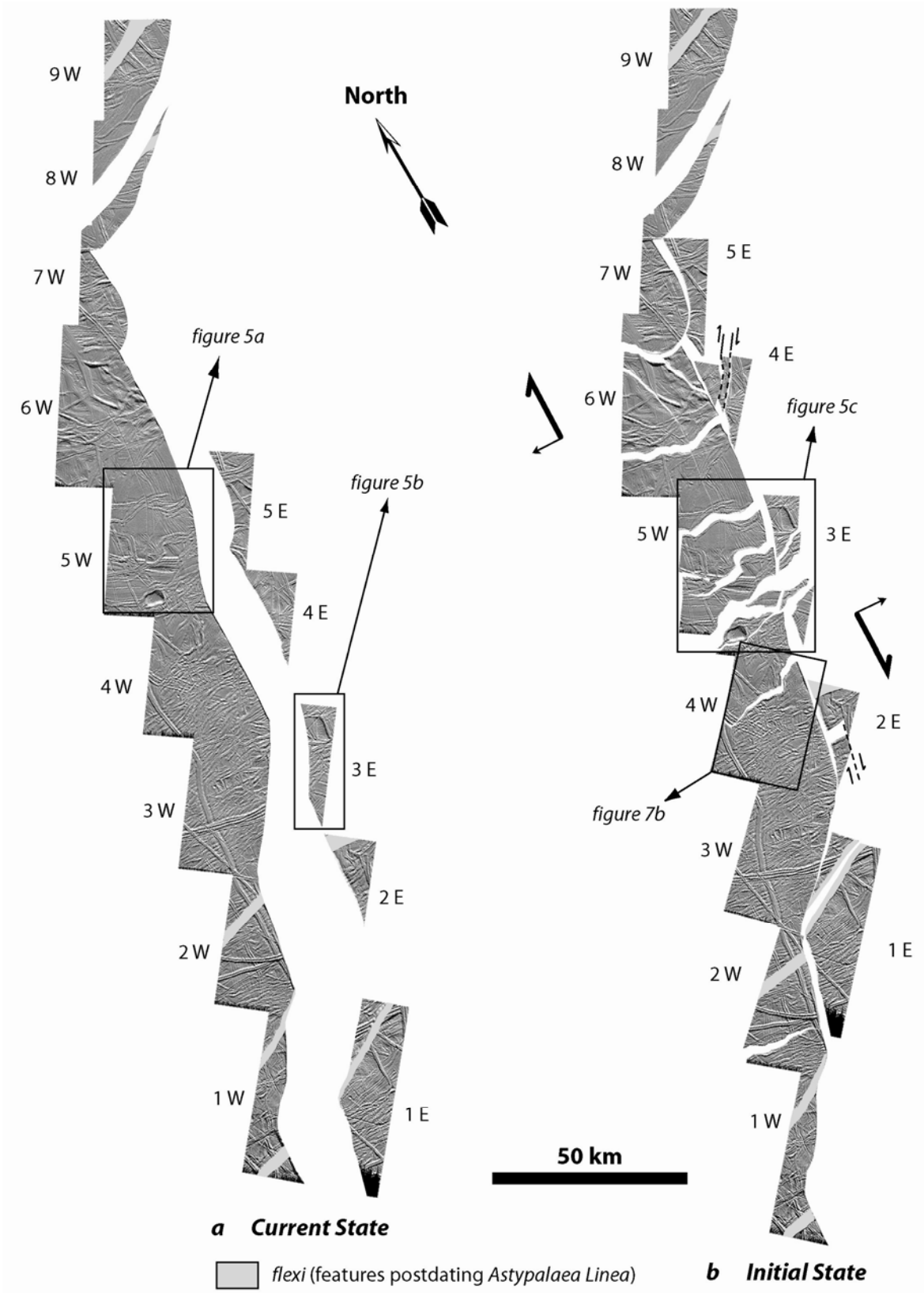


Fig. 6

Comparison between the current surface (a) with the reconstructed initial surface around *Astypalaea Linea* (b). The recent *flexi* are greyed. Textural analysis and piercing points arrangement (as illustrated in fig. 5) require the presence of gaps highlighting disappearance of surface of about 402 km² in the ancient ridged plains.

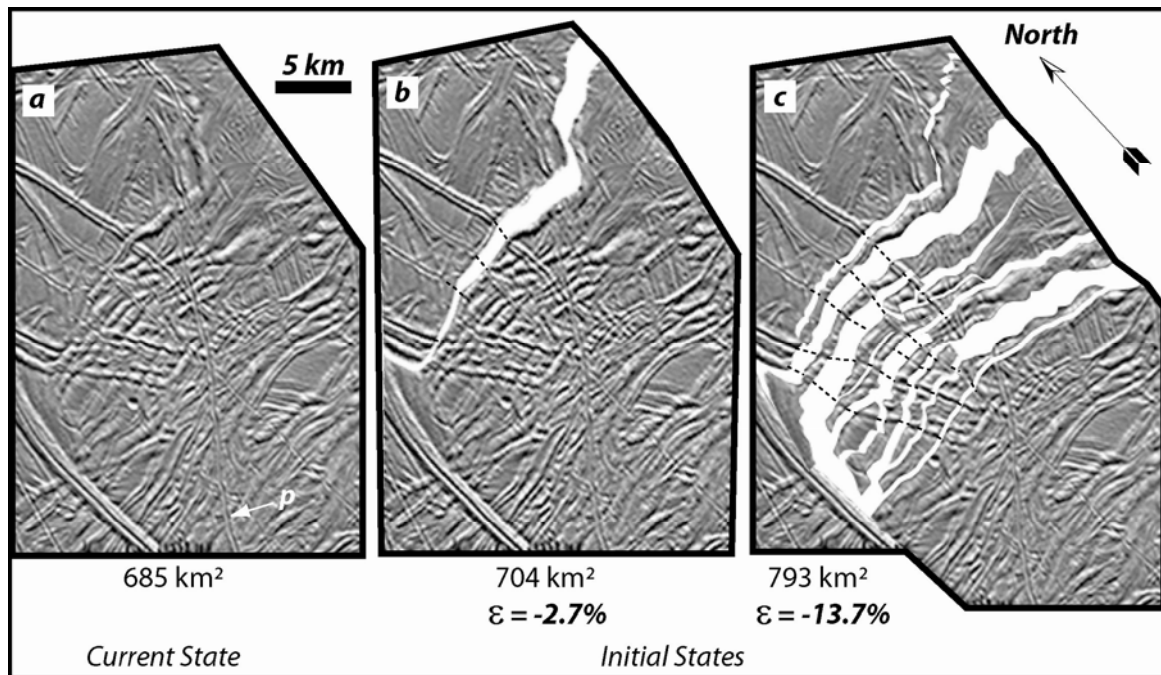


Fig. 7

(a) Detailed analysis of a zone delimited on the fig. 3b and 6b illustrating the scattered character of the compressive deformation. (b) The calculated shortening of this area by using the mosaic reconstruction (fig. 6b) reaches -2.7 %. (c) A more detailed reconstruction provides a better arrangement of the piercing points and the calculated surface shortening reaches -13.7 %. Letter *p* on image *a* indicates a feature postdating *Astypalaea Linea*.

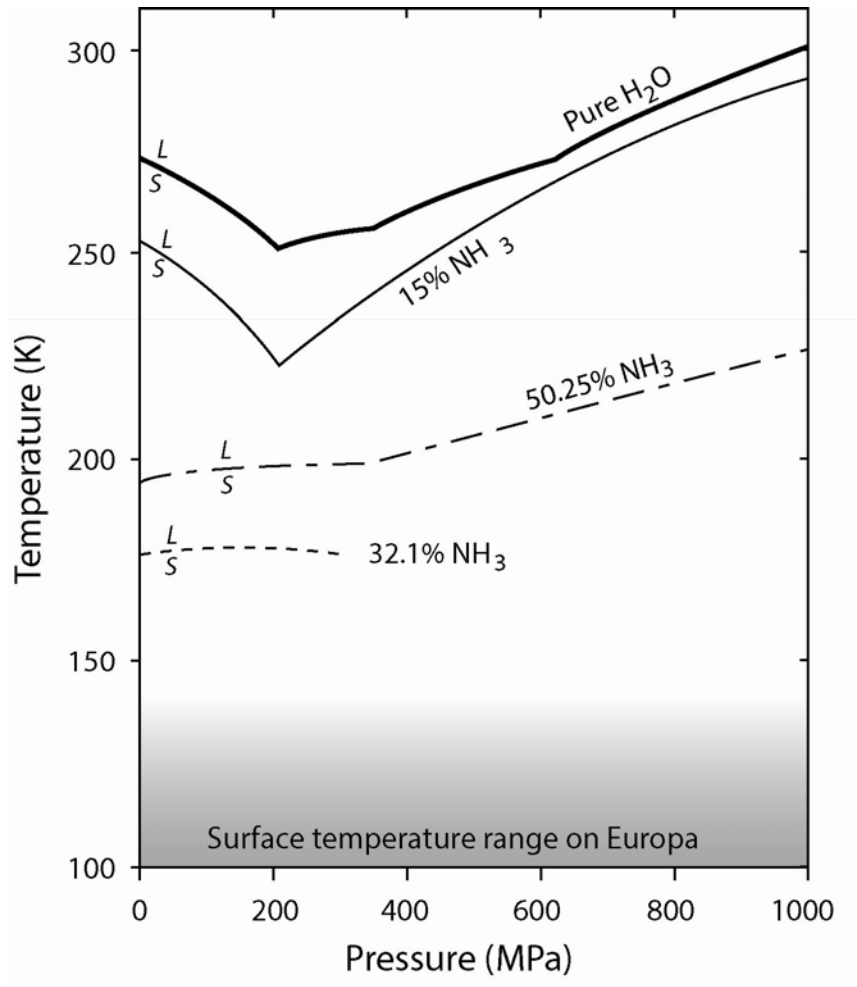


Fig. 8

Pure water phase diagram compared to those of the H₂O-NH₃ system. The (*P-T*) curves represent the liquidus of different ammonia weight per cent mixtures [pure H₂O (Chizhov, 1993), 15 % NH₃ (Grasset et al., 1995), 32.1 % and 50.25 % NH₃ (Hogenboom et al., 1997)]. L and S on each side of the curves refer to liquid and solid states.